

Chiwei Wang · Xiaoling Ma · Jinguo Cheng ·
Jutang Sun · Yunhong Zhou

Synthesis and electrochemical properties of Ca-doped $\text{LiNi}_{0.8}\text{Co}_{0.2}\text{O}_2$ cathode material for lithium ion battery

Received: 23 October 2005 / Revised: 15 February 2006 / Accepted: 21 March 2006 / Published online: 19 April 2006
© Springer-Verlag 2006

Abstract $\text{LiNi}_{0.8}\text{Co}_{0.2}\text{O}_2$ and Ca-doped $\text{LiNi}_{0.8}\text{Co}_{0.2}\text{O}_2$ cathode materials have been synthesized via a rheological phase reaction method. X-ray diffraction studies show that the Ca-doped material, and also the discharged electrode, maintains a hexagonal structure even when cycled in the range of 3.0–4.35 V (vs Li^+/Li) after 100 cycles. Electrochemical tests show that Ca doping significantly improves the reversible capacity and cyclability. The improvement is attributed to the formation of defects caused by the partial occupancy of Ca^{2+} ions in lithium lattice sites, which reduce the resistance and thus improve the electrochemical properties.

Keywords Lithium ion battery · $\text{LiNi}_{0.8}\text{Co}_{0.2}\text{O}_2$ · Ca doping · Defects · Diffusion

Introduction

Lithium ion batteries are considered to be the best available power source for most portable electronic devices, owing to their higher energy density, larger power capacity, and higher working voltage, compared with other secondary batteries [1]. The cycle life and capacity of lithium ion batteries critically depend on the structural and electrochemical properties of the cathode materials. Traditionally, LiCoO_2 is used as commercial cathode material for lithium rechargeable batteries because of its high reversibility, reasonable rate capacity, and easy preparation. However, the toxicity of cobalt coupled with its high cost and low practical capacity limit further applications. Currently, LiNiO_2 is being developed to replace LiCoO_2 , due to the comparatively low cost, high energy density, and environmental advantages of the former. Nevertheless, this material is known to be difficult to synthesize and suffers from instabilities at high states of charge [2, 3]. Therefore, much

research has been undertaken to search for new cathode materials to overcome these shortcomings [4–6].

$\text{LiNi}_{1-x}\text{Co}_x\text{O}_2$ ($0 < x < 1$) compounds, which are isostructural as LiCoO_2 and LiNiO_2 with hexagonal $R\bar{3}m$ α - NaFeO_2 -layered structures and have the advantages of both LiCoO_2 and LiNiO_2 , are considered as promising cathode materials for lithium secondary batteries [7–10]. Elements such as Fe, Al, Y, and Ga have been used for the partial substitution of Ni or Co to further enhance the electrochemical performance of the cathode materials [11–14]. The doped materials showed better structural stability and cycling behavior than the undoped ones. However, the electrochemically inactive dopant generally reduced the reversible cycling capacity.

In the present study, we report an improved reversible capacity and cycling performance of Ca-doped $\text{LiNi}_{0.8}\text{Co}_{0.2}\text{O}_2$ cathode material. The structural and electrochemical properties were investigated to find the reasons for the improvement in electrochemical properties.

Experimental

$\text{LiNi}_{0.8}\text{Co}_{0.2}\text{O}_2$ and Ca-doped $\text{LiNi}_{0.8}\text{Co}_{0.2}\text{O}_2$ cathode materials were synthesized by a rheological phase reaction method [15]. $\text{LiOH} \cdot \text{H}_2\text{O}$, $\text{Ni}(\text{OH})_2$, Co_2O_3 , and $\text{Ca}(\text{OH})_2$ were fully mixed by grinding in a molar ratio of 1:0.8:0.1:0.02. An appropriate amount of deionized water was added to get a rheological body, and the mixture was heated at 80 °C for 2 h in a closed container. After being dried at 120 °C, the mixture was sintered at 730 °C for 10 h in an oxygen atmosphere, and then cooled to room temperature to yield a black product.

The identification of phases and structures was carried out on a Shimadzu 6000 X-ray diffractometer in the 2θ range of 15 to 120°, at a scanning rate of 2°/min and a step of 0.02°, using $\text{Cu K}\alpha_1$ radiation ($\lambda = 1.54056 \text{ \AA}$).

The charge/discharge tests were carried out using the coin-type cell (with a size of 2,016), which consisted of an active-material working electrode and a lithium foil counter electrode separated by a Celgard 2400 microporous mem-

C. Wang · X. Ma · J. Cheng · J. Sun (✉) · Y. Zhou
Department of Chemistry, Wuhan University,
Wuhan 430072, People's Republic of China
e-mail: jtsun@whu.edu.cn
Tel.: +86-27-87218494
Fax: +86-27-68754067

brane. The working electrode was prepared by mixing active material with 15 wt.% acetylene black and 5 wt.% polytetrafluoroethylene binder, compressing the mixture onto an aluminum mesh current collector. A 1 mol/L solution of LiPF_6 dissolved in ethylene carbonate/dimethyl carbonate (DMC) (1:1 volume ratio) was used as the electrolyte. The cells were assembled in an Argon-filled glove box (Mikrouna, Super 1220/750, China). The cells were charged and discharged between 3.0 and 4.35 V (vs Li^+/Li) at different current densities.

Results and discussion

The X-ray diffraction (XRD) patterns of $\text{LiNi}_{0.8}\text{Co}_{0.2}\text{O}_2$ and Ca-doped $\text{LiNi}_{0.8}\text{Co}_{0.2}\text{O}_2$ are shown in Fig. 1. Both compounds show sharp and narrow peaks, indicating a high degree of crystallinity. The patterns can be indexed based on the hexagonal $\alpha\text{-NaFeO}_2$ structure with the $R\text{-}3m$ space group, except a trace amount of CaO peaks as impurity in the spectra of Ca-doped material (Fig. 1b). The spectrum shows a clear split of (006)/(102) and (108)/(110) peaks. According to previous studies [16, 17], the degree of ordering layered structure and the amount of transition metal in the interslab space is indicated from the XRD spectra with the intensity ratios of $I(003)/I(104)$, the c/a ratios of lattice parameters, and the degree of either (108)/(110) or (006)/(102) peak splitting. Crystal lattice parameters of the compounds, which are calculated by means of the least-squares method in terms of hexagonal structure, are given in Table 1. The values of lattice parameters agree well with those reported in literature [18]. Lattice parameters of Ca^{2+} -doped $\text{LiNi}_{0.8}\text{Co}_{0.2}\text{O}_2$ are smaller than those of the undoped material. The ratios of $I(003)/I(104)$ and c/a of Ca^{2+} -doped $\text{LiNi}_{0.8}\text{Co}_{0.2}\text{O}_2$ are larger than those of the undoped material, indicating a better ordering layered structure, as well as a lower degree of cation mixing. This implies that the calcium doping has affected the crystal structure. This may be attributed to the formation of the defects, which occurs from the partial occupancy of Ca^{2+} ions in the lithium lattice sites. A Ca^{2+}

Table 1 Lattice parameters of $\text{LiNi}_{0.8}\text{Co}_{0.2}\text{O}_2$ (a) and Ca-doped $\text{LiNi}_{0.8}\text{Co}_{0.2}\text{O}_2$ (b)

Samples	a (Å)	c (Å)	V (Å ³)	c/a	$I_{(003)}/I_{(104)}$
a	2.8712 (1)	14.1605 (8)	101.0945 (75)	4.9319	1.33
b	2.8656 (1)	14.1564 (7)	100.6705 (80)	4.9401	1.41

ion occupies the Li^+ ion site to form a Ca_{Li} defect and a lithium vacancy (V_{Li}). The formations of the defects shrink the unit cell, suppress the mixing of transition metal in the interslab space, and stabilize the hexagonal $\text{LiNi}_{0.8}\text{Co}_{0.2}\text{O}_2$ structure. The defects in the material would increase the conductivity and diffusion of lithium ions, and thus improve the electrochemical properties [19] (see the discussion of Figs. 3 and 4).

Figure 2 presents the initial charge and discharge curves of $\text{LiNi}_{0.8}\text{Co}_{0.2}\text{O}_2$ and Ca-doped $\text{LiNi}_{0.8}\text{Co}_{0.2}\text{O}_2$ electrodes between 3.0 and 4.35 V at a constant current density of 100 mA/g. Both profiles are similar, indicating similar electrochemical behaviors of the samples. From the figure, we can also observe that Ca-doped $\text{LiNi}_{0.8}\text{Co}_{0.2}\text{O}_2$ has a lower charge voltage than the undoped material at the same charge capacity, while at the same discharge capacity, the former has higher discharge voltage than the latter. Figure 3 shows the cycle performances of the samples. The cathode material of Ca-doped $\text{LiNi}_{0.8}\text{Co}_{0.2}\text{O}_2$ has an initial charge capacity of 212 mAh/g, followed by a discharge capacity of 166 mAh/g. The coulombic efficiency is 78.3%. Even after 100 cycles, the discharge capacity still keeps 163 mAh/g. Only less than 2% of the initial discharge capacity is lost, with an average capacity fade of 0.02% per cycle. In comparison, the $\text{LiNi}_{0.8}\text{Co}_{0.2}\text{O}_2$ material delivers initial charge and discharge capacities of 200 and 153 mAh/g, respectively, with a coulombic efficiency of 76.5%, which is in agreement with the results reported in the literature [10]. The discharge capacity loses 19% in 70 cycles, with an average fade of 0.27% per cycle.

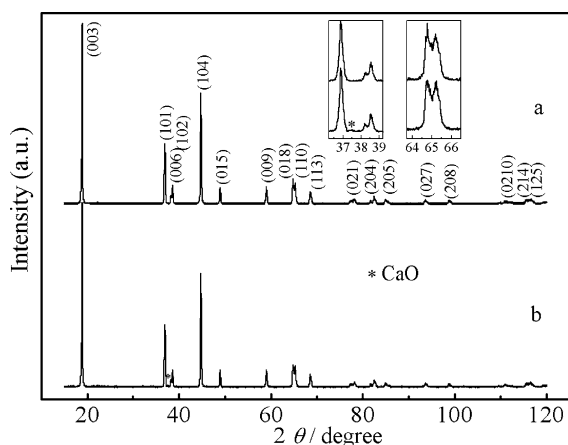


Fig. 1 XRD patterns of compounds: **a** $\text{LiNi}_{0.8}\text{Co}_{0.2}\text{O}_2$, **b** Ca-doped $\text{LiNi}_{0.8}\text{Co}_{0.2}\text{O}_2$

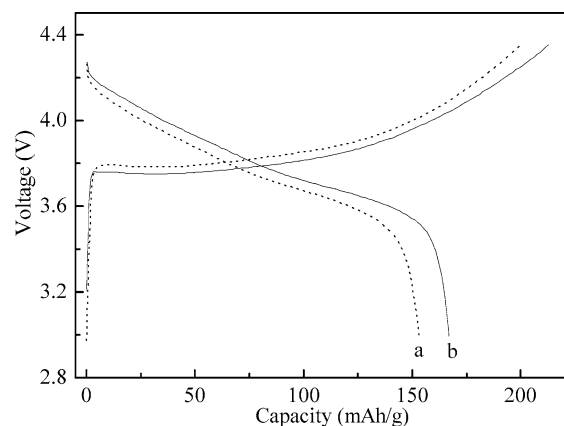


Fig. 2 The initial charge and discharge curves of $\text{LiNi}_{0.8}\text{Co}_{0.2}\text{O}_2$ (a) and Ca-doped $\text{LiNi}_{0.8}\text{Co}_{0.2}\text{O}_2$ (b) electrodes at a current density of 100 mA/g between 3.0 and 4.35 V

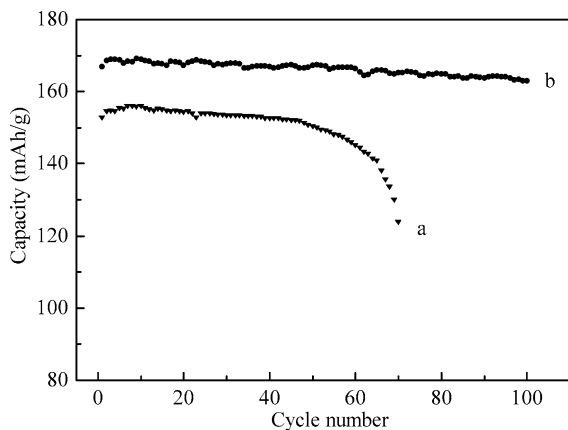


Fig. 3 Cycle performance of $\text{LiNi}_{0.8}\text{Co}_{0.2}\text{O}_2$ (a) and Ca-doped $\text{LiNi}_{0.8}\text{Co}_{0.2}\text{O}_2$ (b) electrodes at a current density of 100 mA/g between 3.0 and 4.35 V

Figure 4 shows the cycle performances of $\text{LiNi}_{0.8}\text{Co}_{0.2}\text{O}_2$ and Ca-doped $\text{LiNi}_{0.8}\text{Co}_{0.2}\text{O}_2$ electrode at a current density of 25 mA/g between 3.0 and 4.35 V. Ca-doped $\text{LiNi}_{0.8}\text{Co}_{0.2}\text{O}_2$ material maintains its initial discharge capacity (174 mAh/g) for up to 30 cycles. By contrast, the undoped material delivers an initial discharge capacity of 169 mAh/g, and the capacity decreases gradually with cycle number. This demonstrates that Ca-doped $\text{LiNi}_{0.8}\text{Co}_{0.2}\text{O}_2$ cathode material has a good rate capacity.

XRD patterns of Ca-doped $\text{LiNi}_{0.8}\text{Co}_{0.2}\text{O}_2$ electrodes discharged at 3.0 V in a voltage range of 3.0–4.35 V after 1 cycle and after 100 cycles are shown in Fig. 5. The discharged electrodes were taken out from the cells and the cathode materials were removed from the aluminum mesh using a doctor blade, washed by DMC and dried under vacuum at 80 °C, and then used for XRD tests. Comparing the XRD patterns, we note that the characteristic peak position of Ca-doped $\text{LiNi}_{0.8}\text{Co}_{0.2}\text{O}_2$ phase maintains unchanged. The ration of $I(003)/I(104)$ remains larger than 1.20, indicating that the material still maintains a good ordering layered structure even after 100 cycles. The sample completely recovers to its initial hexagonal structure after lithium reintercalation.

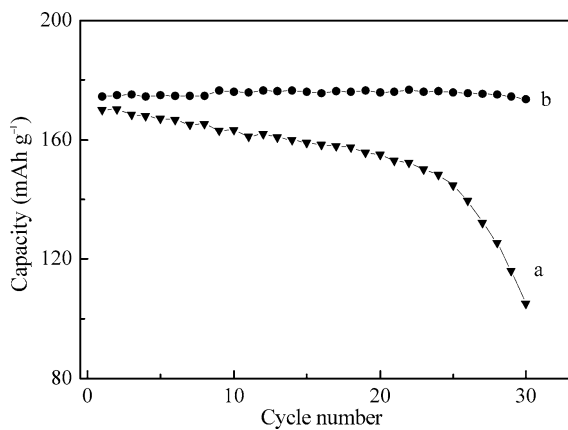


Fig. 4 Cycle performance of $\text{LiNi}_{0.8}\text{Co}_{0.2}\text{O}_2$ (a) and Ca-doped $\text{LiNi}_{0.8}\text{Co}_{0.2}\text{O}_2$ (b) electrodes at a current density of 25 mA/g between 3.0 and 4.35 V

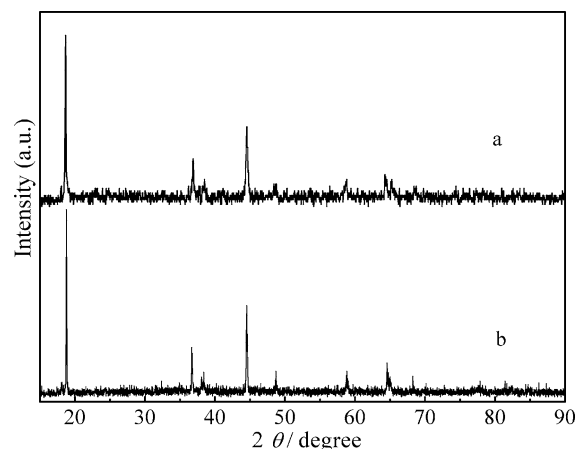


Fig. 5 XRD patterns of a Ca-doped $\text{LiNi}_{0.8}\text{Co}_{0.2}\text{O}_2$ electrode discharged at 3.0 V in voltage range of 3.0–4.35 V: a after 1 cycle and b after 100 cycles

To understand the different cycling characteristics, AC impedance measurements of the two materials were carried out. Figure 6 presents the Nyquist plots obtained at charged state (4.35 V) in the first and fifth cycles. Each plot consists of a depressed semicircle in high and low frequency ranges. The high-frequency semicircle is attributed to the presence of a passivating film on the oxide surface and the low-frequency semicircle to the charge-transfer resistance of electrochemical reaction [20, 21]. The spectra clearly shows that the charge-transfer resistance of Ca-doped $\text{LiNi}_{0.8}\text{Co}_{0.2}\text{O}_2$ electrode is much lower than that of the undoped material, which indicates that the material becomes more conductive with Ca doping. The charge-transfer resistance of the Ca-doped $\text{LiNi}_{0.8}\text{Co}_{0.2}\text{O}_2$ electrode decreased after 5 cycles. By contrast, that of the undoped material increased. The lower resistance is attributed to the effect of Ca which causes the formation of defects (Ca_{Li} and V_{Li}). The defects in the material would increase the conductivity, decrease the activation energy for the hopping of lithium ions from one site to another, and improve the diffusion of lithium ions [19]. From these results, it can be considered that the improved

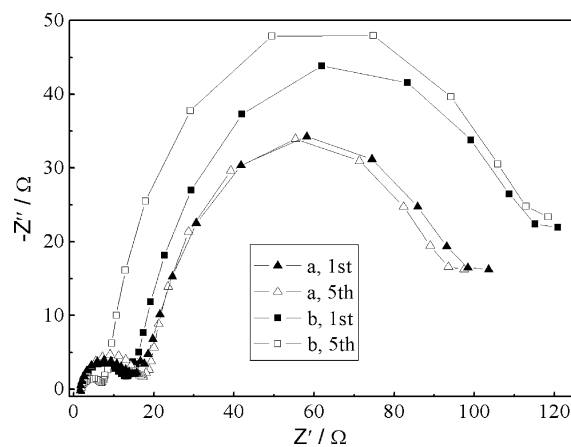


Fig. 6 Nyquist plots of $\text{LiNi}_{0.8}\text{Co}_{0.2}\text{O}_2$ (a) and Ca-doped $\text{LiNi}_{0.8}\text{Co}_{0.2}\text{O}_2$ (b) at charged state (4.35 V) in the first and fifth cycles

electrochemical properties of Ca-doped $\text{LiNi}_{0.8}\text{Co}_{0.2}\text{O}_2$ material were due to the low charge-discharge resistance.

Conclusions

In sum, the effects of Ca doping on the structure and electrochemical properties of $\text{LiNi}_{0.8}\text{Co}_{0.2}\text{O}_2$ powder were investigated. Ca-doped $\text{LiNi}_{0.8}\text{Co}_{0.2}\text{O}_2$ material has smaller lattice parameters and its hexagonal structure maintains even after 100 cycles. It delivers higher reversible capacity and exhibits better cyclability than the undoped material. The superior electrochemical performance of Ca-doped $\text{LiNi}_{0.8}\text{Co}_{0.2}\text{O}_2$ may be ascribed to the reduced resistance.

Acknowledgement This work was supported by the National Natural Science Foundation of China (No. 20471044).

References

1. Tarascon JM, Mckinnon WR, Coowar F, Bowmer TN, Amatucci G, Guyomard D (1994) *J Electrochem Soc* 141:1421
2. Yamada S, Fujiwara M, Kanda M (1995) *J Power Sources* 54:209
3. Ebner W, Fouchard D, Xie L (1994) *Solid State Ion* 68:238
4. Koksang R, Barker J, Shi H, Saidi MY (1996) *Solid State Ion* 84:1
5. Whittingham MS (2004) *Chem Rev* 104:4271
6. Scrosati B (2000) *Electrochim Acta* 45:2461
7. Liu HS, Li J, Zhang ZR, Gong ZL, Yang Y (2003) *J Solid State Electrochem* 7:456
8. Lu CH, Wang HC (2003) *J Mater Chem* 13:428
9. Wu MQ, Chen A, Xu RQ, Li Y (2003) *Mater Sci Eng B, Solid-State Mater Adv Technol* 99:336
10. Ying JR, Wan CR, Jiang CY (2001) *J Power Sources* 102:162
11. Prado G, Fournes L, Delmas C (2001) *J Solid State Chem* 159:103
12. Han CJ, Yoon JH, Cho WI, Jang H (2004) *J Power Sources* 136:132
13. Subba Rao GV, Chowdari BVR, Lindner HJ (2001) *J Power Sources* 97-98:313
14. Balasubramanian M, McBreen J, Pandya K, Amine K (2002) *J Electrochem Soc* 149:A1246
15. Sun JT, Xie W, Yuan LJ, Zhang KL, Wang QY (1999) *Mater Sci Eng B, Solid-State Mater Adv Technol* 64:157
16. Morales J, Vicente CP, Tirado JL (1990) *Mater Res Bull* 25:623
17. Ohuzuku T, Ueda A, Nagayama M (1993) *J Electrochem Soc* 140:1862
18. Gong ZL, Liu HS, Guo XJ, Zhang ZR, Yang Y (2004) *J Power Sources* 136:139
19. Ven AVD, Ceder G (2000) *Electrochem Solid State Lett* 3:301
20. Rodrigues Shalini, Munichandraiah N, Shukla AK (1999) *J Solid State Electrochem* 3:397
21. Nobili F, Croce F, Scrosati B, Marassi R (2001) *Chem Mater* 13:1642